





ACCELERATING MCRT SIMULATIONS USING DIMENSIONALITY REDUCTION TECHNIQUES AND INLA

MAJDA SMOLE¹ , JOÃO RINO-SILVESTRE² ,
SANTIAGO GONZÁLEZ-GAITÁN²  and MARKO STALEVSKI^{1,3} 

¹*Astronomical Observatory, Volgina 7, 11060 Belgrade, Serbia*
E-mail: msmole@aob.rs

²*CENTRA, Instituto Superior Técnico, Av. Rovisco Pais, Lisboa, 1049-001, Portugal*

³*Sterrenkundig Observatorium, Universiteit Gent, Krijgslaan 281-S9, Gent, 9000, Belgium*

Abstract. We propose a post-processing technique for Monte Carlo radiative transfer (MCRT) simulations with a main goal to reduce the total computational run time required for high quality images, by enhancing the output of lower quality images. Our method combines dimensionality reduction techniques with integrated nested Laplace approximation (INLA) to detect and reconstruct the underlying structure in lower quality images or images with missing data. We test the efficiency of our approach using high resolution synthetic observations of Milky Way-sized galaxy from the SKIRT Auriga project. This technique is able to reproduce high-photon-number reference images ~ 5 times faster with median residuals below $\sim 20\%$.

1. INTRODUCTION

Monte Carlo radiative transfer (MCRT) simulations are widely used to investigate dust in astrophysical systems and to generate synthetic observations for simulated galaxies, thus providing a link between numerical simulations and real observations. MCRT simulations are computationally expensive, since they use a large number of photon packages to simulate propagation of photons in realistic 3D inhomogeneous dust distributions (see Noebauer et al. 2019 for a recent review). The SKIRT code is one example of MCRT codes used to simulate the propagation of the radiation through different astronomical environments (Baes & Camps 2015; Camps & Baes 2015).

In this research we introduce a post-processing methodology for enhancing SKIRT simulation output, with the main goal of achieving the quality of high-photon-number images using low-photon-number images as an input. We use dimensionality reduction techniques with the integrated nested Laplace approximation (INLA, Rue et al. 2009; Rue et al. 2017), an approximate method for Bayesian inference to detect and reconstruct the spatial structure of simulated galaxies. In addition to the work presented here (Smole et al. 2022), an alternative approach combines an auto-encoder neural network and INLA (Rino-Silvestre et al. 2022).

In Section METHODS, we introduce our datasets and techniques. In Section RESULTS we present our main findings. In Section SUMMARY, we summarise the results of this work and draw conclusions

2. METHODS

2. 1. INLA

INLA is a computational method for approximate Bayesian inference of latent Gaussian fields, able to use spatial correlations between data points to reconstruct missing and noisy data. We refer to Rue *et al.* (2009) for more details on the mathematical background of INLA.

INLA is available as an R-INLA package designed for modeling spatial data (Rue *et al.* 2017). Since synthetic observations represent non-random spatial structures, we explore the potential of INLA method as a tool to improve MCRT images, and optimize the total computational run time required for high quality images.

2. 2. DIMENSIONALITY REDUCTION TECHNIQUES

In order to achieve additional reduction in computational time, we use principal component analysis (PCA) and non-negative matrix factorisation (NMF) as dimensionality reduction techniques. Both methods transform the original dataset in the spectral dimension, such that in this transformed space, the first components will carry most of the information, while the rest are responsible for less prominent features and noise, and can be discarded in order to trade some of the precision for computational efficiency. Although very similar to PCA, NMF has an additional requirement that both original and decomposed matrices have no negative elements, which might be beneficial when treating data with only non-negative values, such as astronomical fluxes.

2. 3. IMPLEMENTATION

We test the performance of our methodology using high-resolution synthetic images from the SKIRT Auriga project (Kapoor *et al.* 2021). We choose Au-16 galaxy, which represents a typical Milky Way type galaxy with well resolved spiral arms, simulated with three different inclinations (the angle between the angular momentum vector and the direction towards the observer): 'face-on' ($i = 0^\circ$), 'edge-on' ($i = 90^\circ$) and 'intermediate' ($i = 115^\circ$).

These high-resolution synthetic images are the result of a SKIRT simulation performed with 3×10^{10} photon packages, which are hereafter referred to as the high photon number (HPN) reference images. In addition, we ran simulations of the same galaxy, but with a lower number of photon packages, 3×10^8 and 3×10^9 , and used them as low photon number (LPN) input images. LPN input images require only $\sim 2\%$ and $\sim 11\%$ of the HPN reference simulation execution time for 3×10^8 and 3×10^9 photon packages, respectively.

However, INLA spacial reconstructions alone can also be time costly, especially for large data cubes (of 50 wavelengths) such as in this particular case. Such reconstructions are labelled 'pure INLA' in the following text. We employed PCA and NMF techniques to reduce the number of wavelength dimensions to 10 principal components. In that way we reduce the number of individual spatial maps to be reconstructed with INLA. Such reconstructions are labelled 'PCA or NMF with INLA' reconstructions.

Additionally, the INLA spatial reconstruction time can be reduced by sampling the input map data, instead of using complete spatial information. INLA shows optimal

performance when applied to sparse data, the execution time is notably reduced, while the quality of reconstructions is influenced only to a lesser degree. We perform tests to find an optimal sampling percentage and optimal number of PCA or NMF components.

3. RESULTS

In this section, we present the results using pure INLA and PCA or NMF with INLA techniques. We test our method using LPN SKIRT simulations (3×10^8 and 3×10^9 photon packages) with different inclination angles: face-on, edge-on, and intermediate. INLA reconstructions are performed using 10% or 25% of the available spatial information, and 10 PCA or NMF components. Table 1 summarises the results. The quality of INLA reconstructions, compared to HPN reference images, is quantified by the normalised residuals:

$$\text{Residuals (\%)} = \left| \frac{X' - X}{X} \right| \times 100\%, \quad (1)$$

where X' and X refer to INLA reconstruction and HPN reference images, respectively. Running times presented in Table 1 are as follows:

$$t (\%) = \frac{t_{\text{LPN SKIRT}} + t_{\text{INLA}}}{t_{\text{HPN SKIRT}}} \times 100\%, \quad (2)$$

where t_{INLA} refers either to pure INLA reconstructions or to the total time for PCA or NMF analysis with INLA reconstructions.

For each realisation, residuals for our reconstructions are significantly lower compared to LPN input residuals, proving that each of the employed methods is able to recover spatial structure using only 10% or 25% of the LPN input. Although pure INLA reconstructions result in the lowest residuals, this methodology does not provide a significant acceleration. However, employing dimensionality reduction techniques successfully reduces the running times for up to $\sim 10\%$ of HPN reference's with similar residuals. Depending on the LPN input and the sample size, residuals of PCA or NMF with INLA reconstructions are in the range of $\sim 10\text{-}20\%$ for the face-on cube and $\sim 15\text{-}30\%$ for the edge-on and intermediate cubes.

Next, we explore how the quality of our reconstructions changes at different regions throughout the galaxy plane. We inspected SEDs for individual spaxels, where spaxel refers to spectral pixel, with a spectrum associated with each one. The chosen spaxels occupy different regions of galaxy morphology, such as central parts, strong spiral arms, low flux density regions between spiral arms and galaxy outskirts. Figure 1 shows single-spaxel SEDs for intermediate cubes, sampling 25% of 3×10^8 photon number realisation. Both pure INLA (green) and PCA or NMF with INLA (blue and cyan lines) reconstructions are generally in good agreement with HPN reference SEDs (black lines) for most pixel positions. The quality of reconstructions is correlated with the spaxel position and the flux density. At high flux density regions, such as central parts and prominent spiral arms, LPN input SEDs (red lines) closely follow the HPN reference, and each of the employed techniques provides accurate predictions (spaxels at positions 1 and 2). At lower flux densities along spiral arms (spaxels 3 and 4), the LPN input becomes noisy; however, the quality of our reconstructions is not affected.

Table 1: Median of the normalised residuals and the running times, compared to HPN reference.

angle	LPN input			pure INLA		PCA+INLA		NMF+INLA	
	photon number	median (%)	input sample	median (%)	time (%)	median (%)	time (%)	median (%)	time (%)
face-on	3×10^9	17.68	25%	9.97	110	10.68	32	11.35	40
	3×10^8	60.97	10%	11.61	89	12.21	26	12.79	35
			10%	15.57	103	15.46	27	17.65	24
edge-on	3×10^9	30.23	25%	13.36	58	20.62	18	15.85	24
	3×10^8	96.88	10%	15.67	43	22.54	15	17.5	20
			10%	23.42	47	31.18	10	24.92	12
inter-mediate	3×10^9	24.91	25%	29.38	28	35.28	7	27.47	8
	3×10^8	86.13	10%	12.10	97	12.63	24	12.73	33
			10%	14.57	76	14.41	21	14.51	26
			10%	20.03	89	19.27	22	23.00	22
			10%	25.10	66	22.63	13	25.89	16

Yet, the reconstruction of the faint, outermost parts of the galaxy (spaxels 5 and 6) becomes challenging given the LPN input SEDs with both noisy and missing data. In these regions, pure INLA and NMF with INLA are, overall, able to recover the full SED of the HPN reference cube, while PCA with INLA occasionally fails in the reconstruction, resulting in non-physical negative flux densities. Such an example is shown in spaxel 5 of Figure 1, where the LPN input spaxel is not complete, meaning it has zero values at some wavelengths.

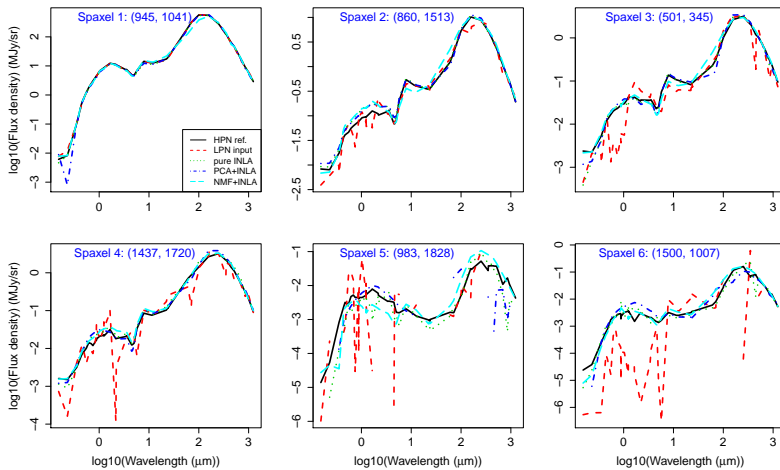


Figure 1: Single-spaxel SEDs for HPN reference (black) and LPN input (red) intermediate cubes, together with pure INLA (green) and PCA or NMF with INLA (blue and cyan) reconstructions.

Figure 2 shows spatial distribution of randomly sampling 25% of the LPN input cube spaxels, together with pure INLA and PCA or NMF with INLA reconstructions (upper panels) at a wavelength bin of $7.88 \mu\text{m}$. Each of these cubes is compared to the HPN reference and normalised residuals are shown in the lower panels. By using

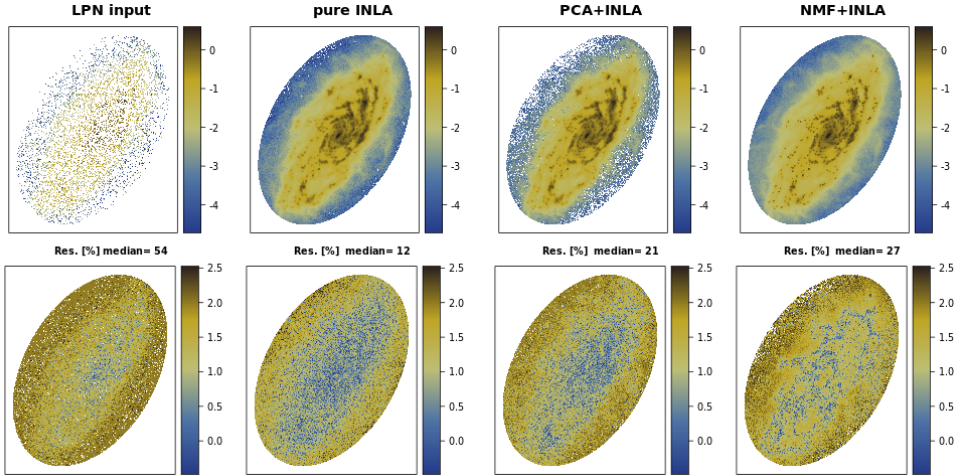


Figure 2: Spatial distribution of LPN input cube and pure INLA, PCA or NMF with INLA reconstructions (upper panels) with the associated residuals (bottom panels) at wavelength bin $7.88 \mu\text{m}$. Sample size: 25%, intermediate cube. Colour legends are given in logarithmic scale

a sample of LPN input cubes our methods are able to recover underlying spatial information and reveal structures. The quality of reconstructions is quantified by the median of normalised residuals (%), calculated for each pixel at the given wavelength bin, and shown above each residual reconstruction image. The pure INLA results generally have the lowest residuals; however, this technique has an extensive running time. The PCA or NMF with INLA reconstructions have similar residuals, with $< 25 \%$ of the running time required for HPN reference (Table 1). However, at certain wavelength bins, the PCA with INLA technique fails in the reconstruction of $\sim 10\%$ of the spatial information, positioned at regions with the lowest flux density. Those regions with non-physical negative flux densities can be seen in Figure 2 as white pixels. The problem with non-physical reconstructions induced by PCA analysis can be avoided using NMF instead, since NMF always provides physically positive reconstructions. Using the NMF with INLA method, the problematic regions are reconstructed, but with typically higher residuals compared to pure INLA. However, PCA analysis has advantages over NMF: PCA analysis is faster, and the number of PCA components does not need to be decided in advance. Thus, masking out the outskirt regions prior to INLA would improve the reconstructions.

4. SUMMARY

In this work (Smole et al. 2022), we used PCA and NMF dimensionality reduction techniques with INLA for post-processing of LPN SKIRT simulations. We tested our methodology using three images of the Au-16 SKIRT Auriga galaxy, simulated with different tilt angles: face-on, edge-on, and intermediate. These HPN reference images (3×10^{10} photon packages) served as the 'ground truth' to which we compared the performance of our method applied to LPN input images (3×10^8 or 3×10^9 photon packages).

Depending on the number of photon packages, the sample size, and the desired quality of reconstruction, our method offers time-efficient reconstructions with spatial residuals of $\sim 20 - 30\%$, requiring $\sim 7 - 20\%$ of the HPN reference running time. Higher quality reconstructions can be achieved by sampling 25% of the 3×10^9 LPN input image, resulting in residuals of $\sim 10 - 20\%$ within $\sim 20 - 40\%$ of the HPN reference running time.

The proposed technique provides a tool to efficiently perform large number of LPN simulations with various parameters, and such analyses can serve to narrow down the parameters to then run a full HPN simulation.

Acknowledgements

We acknowledge the support by the programme of scientific and technological cooperation between the government of the Republic of Serbia and the government of the Republic of Portugal, (grant No. 337-00-00227/2019-09/53 and FCT 5581 DRI, Sérvia 2020/21). M.S. and M.S. acknowledge support by the Science Fund of the Republic of Serbia, PROMIS 6060916, BOWIE and by the Ministry of Science, Technological Development and Innovation of the Republic of Serbia (MSTDIRS) through contract no. 451-03-66/2024-03/200002 made with Astronomical Observatory of Belgrade. J. R.-S. is funded by Fundação para a Ciência e a Tecnologia (PD/BD/150487/2019), via the International Doctorate Network in Particle Physics, Astrophysics and Cosmology. S.G.G and J.R.-S. acknowledge the support of FCT under Project CRISP PTDC/FIS-AST-31546/2017.

References

- Baes, M., Camps, P.: 2015, *Astronomy and Computing*, **12**, 33
Camps, P., Baes, M.: 2015, *Astronomy and Computing*, **9**, 20
Kapoor, A. U., Camps, P., Baes, M., et al.: 2021, *MNRAS*, **506**, 5703
Noebauer, U. M., Sim, S. A.: 2019, *Living Reviews in Computational Astrophysics*, **5**, 1
Rino-Silvestre, J., González-Gaitán, S., Stalevski, M., et al.: 2022, *Neural Computing and Applications*, **35**, 7719
Rue, H., Martino, S., Chopin, N.: 2009, *Journal of the Royal Statistical Society: Series B (Statistical Methodology)*, **71**, 319
Rue, H., Riebler, A., Sørbye, S.H., Illian, J.B., Simpson, D.P., Lindgren, F.K.: 2017, *Annual Review of Statistics and Its Application*, (4), 395
Smole, M., Rino-Silvestre, J., González-Gaitán, S., Stalevski, M.: 2022, *A&A*, **669**, 152